Reports

Imaging Powders with the Atomic Force Microscope: From Biominerals to Commercial Materials

GERNOT FRIEDBACHER,* PAUL K. HANSMA, EMANNUEL RAMLI, GALEN D. STUCKY†

Atomically resolved images of pressed powder samples have been obtained with the atomic force microscope (AFM). The technique was successful in resolving the particle, domain, and atomic structure of pismo clam (*Tivela stultorum*) and sea urchin (*Strongylocentrotus purpuratus*) shells and of commercially available calcium carbonate ($CaCO_3$) and strontium carbonate ($SrCO_3$) powders. Grinding and subsequent pressing of the shells did not destroy the microstructure of these materials. The atomic-resolution imaging capabilities of AFM can be applied to polycrystalline samples by means of pressing powders with a grain size as small as 50 micrometers. These results illustrate that the AFM is a promising tool for material science and the study of biomineralization.

THE ATOMIC FORCE MICROSCOPE (AFM) (*1, 2*) has been used to image conductors (*3*), nonconductors (*4*), and polymers (*5*) and to study friction (*6*), magnetic fields (*7*), and chemical processes (*8, 9*) with atomic resolution. All of these studies have used relatively large (~500 μm or greater) flat surfaces. This approach precludes the characterization of many important materials, for example, metastable zeolite catalyst microcrystals (~5 μm or less) and semicrystalline or polycrystalline phases formed in biomineralization chemistry. The AFM also could be used to study the role of proteins in biomineralization processes, which are of considerable interest (*10*). Moreover, there is no principal limitation for studying in situ processes, since imaging is also possible under liquids. Implementation of polycrystalline sample preparation techniques can greatly enhance the analytical scope and applicability of AFM.

We report particle, domain, and atomic structures of pismo clam (*Tivela stultorum*) and sea urchin (*Strongylocentrotus purpuratus*) shells obtained by polycrystalline AFM techniques. Commercial $CaCO_3$ and $SrCO_3$ powders were also investigated for comparison with the shell samples and to demonstrate the atomic-resolution imaging capabilities of AFM on "off-the-shelf" chemicals. The structure, both on the atomic and the micrometer scale, of calcitic $CaCO_3$ powder (from commercial $CaCO_3$ and from the sea urchin shell) was revealed by the AFM to be different from the aragonitic powder (from $SrCO_3$ and from the clam shell).

All of the measurements were carried out with a Nanoscope II AFM (*11*) interfaced to a personal computer. The detection scheme of this instrument is based on laser beam deflection off a microfabricated cantilever. Further details and references are given in a recent review (*12*).

The pismo clam shells were collected at Pismo Beach, California. Their size was ~10 cm in diameter. It is known that $CaCO_3$ constitutes 98 to 99% of the inorganic material of sea shells (*13*). The powder x-ray diffraction pattern of that particular shell was congruent with that of pure aragonite. Sea urchin shells were obtained at Goleta Beach, California. Powder x-ray diffraction showed that the material contains calcite only. Powder pellets of the shells were obtained by grinding fractured pieces with an alumina mortar and pestle until a powder with a grain size of ~50 μm was obtained. Approximately 0.5 g of the ground powder was then loaded into a KBr die (Perkin-Elmer) and pressurized at 5×10^8 Pa for 15 min with a Carver laboratory press. Pellets of 13 mm in diameter and 1.5 mm in thickness were obtained. Calcitic $CaCO_3$ (ACS primary standard, Alfa) and aragonitic $SrCO_3$ (99%, Aldrich) powders were pressed into pellets under the same conditions.

The powder x-ray diffraction patterns of the pressed samples were identical with those obtained from the untreated powders and did not indicate any structural modification. In principle such modifications are possible if grinding and pressing is carried out under conditions described in (*14*). We show, however, that our process of sample preparation did not destroy the original structure of the samples. Localized pressing artefacts could be investigated by the AFM, although this was not our goal.

A micrometer-scale AFM image of the untreated inner surface of a shell is shown in Fig. 1A. The image clearly reveals a layered, overlapping platelet structure, where the size of the most visible parts of the platelets is in the range of 0.5 μm. Measurements on different parts of the sample confirmed that this structure is reproducible and representative.

Next we compared the structure seen on the untreated sample with that observed on a pellet of pressed powder of the same material imaged at a higher magnification (Fig. 1B). The particular microstructure of the material shown in the previous image (Fig. 1A) was not destroyed by the rough

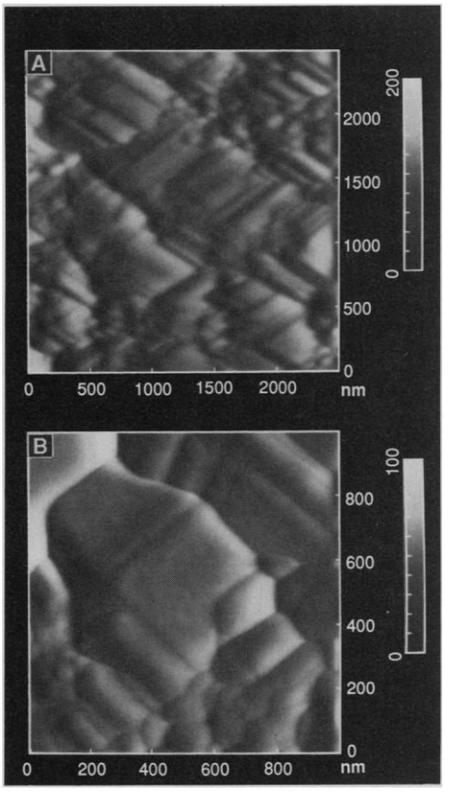

Fig. 1. (**A**) An AFM image of an untreated surface of a *T. stultorum* shell. Imaged field, 2500 nm by 2500 nm; depth scale, 200 nm from black to white. (**B**) An AFM image of a pressed powder sample of *T. stultorum* shells. Imaged field, 1000 nm by 1000 nm; depth scale, 100 nm from black to white.

G. Friedbacher and P. K. Hansma, Department of Physics, University of California, Santa Barbara, CA 93106.
E. Ramli and G. D. Stucky, Department of Chemistry, University of California, Santa Barbara, CA 93106.

*Permanent address: Institute for Analytical Chemistry, Technical University Vienna, Getreidemarkt 9/151, A-1060 Wien, Austria.
†To whom correspondence should be addressed.

treatment of the sample. It is an interesting and important finding that reproducible AFM imaging on a pressed powder pellet is possible in a straightforward manner: the finding suggests a new sample preparation technique that can widen the variety of materials that can be investigated with the AFM. In principle, samples of any geometry could be transferred to the geometrical form of a pellet and analyzed. It should also be emphasized that there is no limitation for nonconducting samples: no coating is necessary.

An atomically resolved image of the pressed powder (Fig. 1B) is shown in Fig. 2A. Computer simulations (*15*) of several aragonite planes suggested that we are observing either the (011) plane (Fig. 2B) or the (001) plane. Calculated angles and bond distances for both planes are in agreement with the experimental values within the accuracy of AFM (~10%). Distortions seen in AFM images are mainly due to the calibration of the piezo scanner and thermal drifts. Similar images can be obtained by zooming in on the platelets. An atomically resolved image of a $SrCO_3$ powder pellet is shown in Fig. 2C. This sample, which has the aragonite structure, shows a pattern indicative of the (011) or (001) planes and is similar to the one obtained on the shell.

A micrometer-scale image of the pressed $CaCO_3$ sample is shown in Fig. 3. Atomically resolved images from that sample (Fig. 4A) have been obtained by zooming in at the center of particles. A similar image of atoms on the sea urchin sample is shown in Fig. 4B. Here, computer simulations of several calcite planes suggested that in both cases we are observing the (001) plane (Fig. 4C). It should be stressed that we do not rule out the existence of other planes on other crystallites in our pellet.

Our study has shown that the described process of grinding and pressing of our samples did not destroy their original microstructure, and that it was an appropriate treatment to simplify subsequent imaging to the atomic scale. Moreover, images of the commercial $CaCO_3$ and $SrCO_3$ samples demonstrated that off-the-shelf chemicals could be imaged readily. As an extension of this study, we have been successful at imaging concrete materials at an atomic resolution.

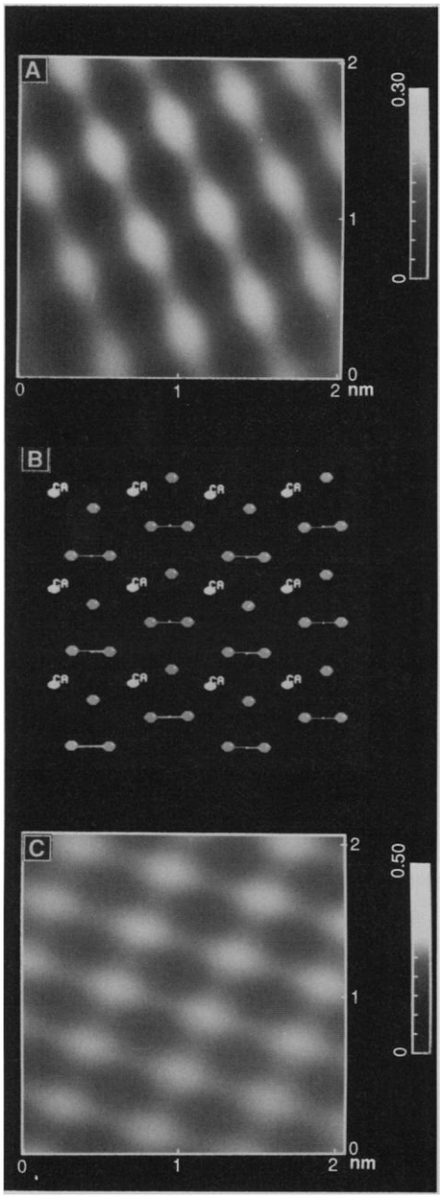

Fig. 2. (**A**) Atomically resolved AFM image of a pressed powder sample of *T. stultorum* shells. Imaged field, 2 nm by 2 nm; depth scale, 0.3 nm from black to white. Image filtered by means of a two-dimensional Fourier transform. Spacings, 4.6 and 6.1 Å, respectively; angle, 88°. (**B**) Chem-X computer simulation of an aragonite (011) plane with the use of the *Pnma* space group. Calcium atoms are bright, and oxygen atoms are dark. The calculated distances between the Ca atoms, which form one layer parallel to the (011) plane, are 4.70 and 5.74 Å, respectively; the angle is 88.6°. [The (001) Ca-Ca spacings are 4.96 and 5.74 Å; angle, 90°.] (**C**) Atomically resolved AFM image of a pressed $SrCO_3$ powder sample; imaged field, 2.07 nm by 2.07 nm, depth scale, 0.5 nm from black to white. Spacings, 4.3 and 6.2 Å, respectively; angle, 84°.

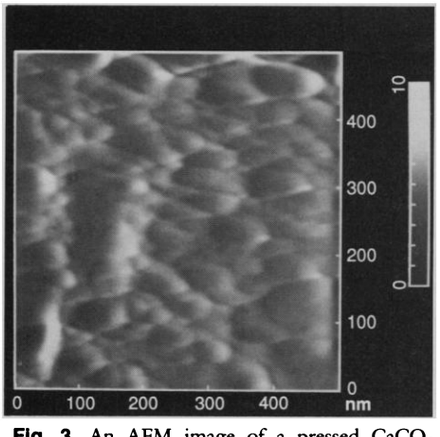

Fig. 3. An AFM image of a pressed $CaCO_3$ powder. Imaged field, 500 nm by 500 nm; depth scale, 10 nm from black to white.

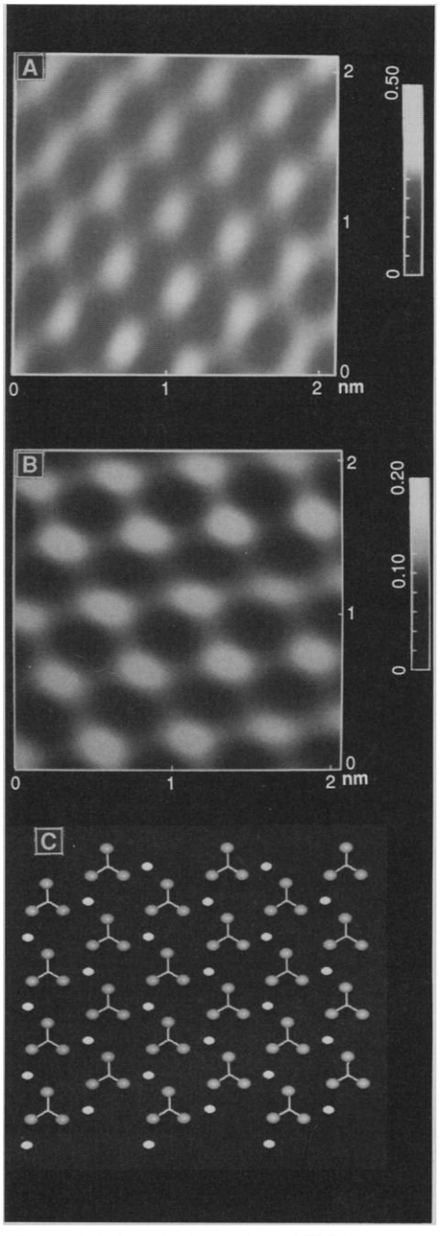

Fig. 4. (**A**) Atomically resolved AFM image of a pressed $CaCO_3$ powder sample. Imaged field, 2.1 nm by 2.1 nm; depth scale, 0.5 nm from black to white. Image filtered by means of a two-dimensional Fourier transform. Spacings, 5.0, 5.2, and 4.5 Å, respectively; angles, 60°, 66°, and 54°, respectively. (**B**) Atomically resolved AFM image of a pressed powder sample of (*S. purpuratus*) shells. Imaged field, 2.1 nm by 2.1 nm; depth scale, 0.2 nm from black to white. Spacings, 5.4, 5.4, and 4.8 Å, respectively; angles, 62°, 55°, and 63°. (**C**) Chem-X computer simulation of a calcite (001) plane with the use of the $R\bar{3}c$ space group and showing one layer of calcium cations and of carbonate anions. The calculated distance between the Ca atoms (bright) is 4.99 Å. Oxygen atoms are dark.

REFERENCES AND NOTES

1. G. Binnig, C. F. Quate, Ch. Gerber, *Phys. Rev. Lett.* **56**, 930 (1986).
2. P. K. Hansma, V. B. Elings, O. Marti, C. E. Bracker, *Science* **242**, 209 (1988).
3. G. Binnig, Ch. Gerber, E. Stoll, T. R. Albrecht, C. F. Quate, *Europhys. Lett.* **3**, 1281 (1987).
4. T. R. Albrecht and C. F. Quate, *J. Appl. Phys.* **62**, 2599 (1987).
5. T. R. Albrecht *et al.*, *ibid.* **64**, 1178 (1988).
6. C. M. Mate, G. M. McClelland, R. Erlandsson, S. Chiang, *Phys. Rev. Lett.* **59**, 1942 (1987).
7. Y. Martin and H. K. Wickramasinghe, *Appl. Phys. Lett.* **50**, 1455 (1987).
8. S. Alexander *et al.*, *J. Appl. Phys.* **65**, 164 (1989).
9. B. Drake *et al.*, *Science* **243**, 1586 (1989).
10. D. D. Lee, *J. Cryst. Growth* **102**, 262 (1990); L. Pach *et al.*, *J. Mater. Res.* **5**, 2928 (1990); S. Mann, *Nature* **332**, 119 (1988); ———, B. R. Heywood, S. Rajam, J. D. Birchall, *ibid.* **334**, 692 (1988); L. Addadi and S. Weiner, *Proc. Natl. Acad. Sci. U.S.A.* **82**, 4110 (1985); A. Berman, L. Addadi, S. Weiner, *Nature* **331**, 546 (1988); A. Berman *et al.*, *Science* **250**, 664 (1990); J. D. Birchall, *Trans. J. Br. Ceram. Soc.* **83**, 158 (1984).
11. Digital Instruments, 6780 Cortona Drive, Santa Barbara, CA 93117.
12. D. Rugar and P. Hansma, *Phys. Today* **43** (no. 10), 23 (1990).
13. J. A. C. Nicol, *The Biology of Marine Animals* (Interscience, New York, 1960), p. 646.
14. H. R. Wenk, D. J. Barber, R. J. Reeder, in *Reviews in Mineralogy*, R. J. Reeder, Ed. (Mineralogical Society of America, Washington, DC, 1983), vol. 11, pp. 301–367; F. Dachille and R. Roy, *Nature* **186**, 34 (1960); J. H. Burns and M. A. Bredig, *J. Chem. Phys.* **25**, 1281 (1956); R. Schrader and Br. Hoffmann, *Z. Chem.* **6**, 388 (1966).
15. Simulations were done with Chem-X, developed and distributed by Chemical Design Ltd., Oxford, England. The simulations were constructed based on published x-ray diffraction parameters (lattice parameters, atomic coordinates, and space groups). Crystallographic parameters for simulating the aragonite structure were from A. Dal Negro and L. Ungaretti, *Am. Mineral.* **56**, 768 (1971). Those for the calcite structure were from H. Chessin and W. C. Hamilton, *Acta Crystallogr.* **18**, 689 (1965).
16. Support of this work by the National Science Foundation, Solid State Physics grants no. DMR 89-17164 (P.K.H.) and no. DMR 88-21499 (G.D.S.), the Austrian Fonds zur Förderung der Wissenschaftlichen Forschung (G.F.), and Concrete Technology Corp. (E.R. and G.D.S.) is gratefully acknowledged. Purchases and building of AFM equipment were supported in part by the Office of Naval Research and Digital Instruments.

11 February 1991; accepted 10 July 1991

The Dark Side of Venus: Near-Infrared Images and Spectra from the Anglo-Australian Observatory

D. CRISP,* D. A. ALLEN, D. H. GRINSPOON,† J. B. POLLACK

Near-infrared images and spectra of the night side of Venus taken at the Anglo-Australian Telescope during February 1990 reveal four new thermal emission windows at 1.10, 1.18, 1.27, and 1.31 micrometers (μm), in addition to the previously discovered windows at 1.74 and 2.3 μm. Images of the Venus night side show similar bright and dark markings in all windows, but their contrast is much lower at short wavelengths. The 1.27-μm window includes a bright, high-altitude O_2 airglow feature in addition to a thermal contribution from the deep atmosphere. Simulations of the 1.27- and 2.3-μm spectra indicate water vapor mixing ratios near 40 ± 20 parts per million by volume between the surface and the cloud base. No large horizontal gradients in the water vapor mixing ratios were detected at these altitudes.

ALLEN AND CRAWFORD (*1*) DISCOVered that the night side of Venus is surprisingly bright at near-infrared (NIR) wavelengths between 1 and 3 μm. Their spectroscopic measurements revealed emission peaks near 1.74 and 2.3 μm, in the relatively transparent spectral windows between CO_2 and H_2O absorption bands in the Venus atmosphere, where the planet-wide sulfuric acid (H_2SO_4) clouds provide the principal source of opacity. NIR images of the night side of Venus show bright and dark markings that move from east to west with rotation periods between 5 and 7 days. This night-side emission is produced by hot gases in the lower atmosphere of Venus, below the H_2SO_4 cloud deck (*2, 3*). The NIR markings are formed as this radiation passes through regions of the clouds that have different optical depths (*3*).

Analyses of NIR spectra have provided improved estimates of the concentrations of important trace gases in the deep atmosphere including H_2O, HDO, CO, and OCS (*4, 5*). Most NIR spectra (*2, 4, 5*) indicate water vapor mixing ratios near 40 parts per million by volume (ppmv) at altitudes between 30 and 50 km. Only one NIR spectrum (*5*) indicates much larger amounts of water (200 ppmv) similar to those inferred from entry probe measurements (*6, 7*). The limited spatial sampling provided by these NIR spectra does little to constrain the global distribution of H_2O below the clouds, but, if the dry conditions indicated by most of these spectra prevail throughout the deep atmosphere, they have important implications for the atmospheric evolution and the efficiency of the greenhouse mechanism that maintains the high surface temperatures. Comparisons between the H_2O and HDO abundances derived from NIR spectra confirm that the Venus atmosphere has lost a substantial amount of H_2O since its formation (*4*). With such losses, small H_2O amounts similar to those detected in most NIR spectra may have atmospheric lifetimes shorter than the age of the solar system (*8*). These arguments suggest that the present H_2O amounts may be maintained by a steady-state influx from volcanoes or comets. They also preclude the need for a large primordial water inventory. This, in turn, weakens current theories on the origin and evolution of the massive CO_2 atmosphere and the high surface temperatures on Venus, because large H_2O amounts play a vital role in the primordial "runaway greenhouse" that is thought to have produced these conditions (*9*).

These NIR observations also raise questions about the present-day greenhouse

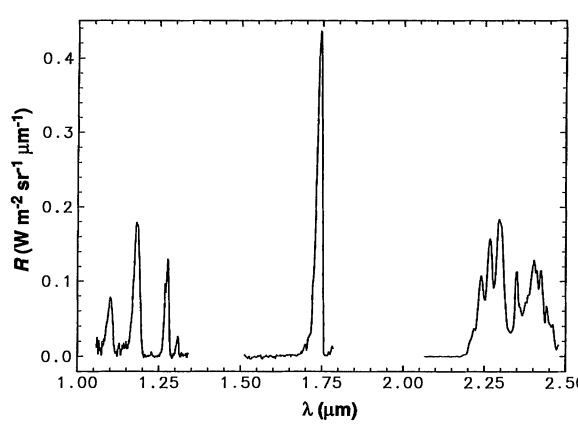

Fig. 1. Radiance R plotted as a function of wavelength λ for a low-resolution spectrum ($\lambda/\Delta\lambda \sim 600$) of a bright region on the night side of Venus from 10 February 1990. The new thermal emission windows at 1.10, 1.18, 1.27, and 1.31 μm are shown as well as the previously discovered 1.74- and 2.3-μm features.

D. Crisp, MS 169-237, Jet Propulsion Laboratory, California Institute of Technology, 4800 Oak Grove Drive, Pasadena, CA 91109.
D. A. Allen, Anglo-Australian Observatory, Post Office Box 296, Epping, New South Wales, 2121, Australia.
D. H. Grinspoon and J. B. Pollack, MS 245-3, National Aeronautics and Space Administration (NASA) Ames Research Center, Moffett Field, CA 94035.

*To whom correspondence should be addressed.
†Present address: Laboratory for Atmospheric and Space Physics, University of Colorado, Boulder, CO 80309.